https://doi.org/10.16886/IAS.2025.03

SEBASTIAN YEREX¹, BRYNDÍS MARTEINSDÓTTIR², RÁN FINNSDÓTTIR², NOÉMIE BOULANGER-LAPOINTE¹

¹Department of Geography, University of Victoria, Victoria, BC V8P 5C2, Canada, ²Land and Forest Iceland, Gunnarsholt, 851 Hella, Iceland

ABSTRACT

Vegetation cover exerts a strong influence on the rate and severity of soil erosion. In Iceland, soil erosion is a major land management issue, with accelerating rates of degradation since human occupation. Current methods for erosion mapping and monitoring are costly and difficult to employ frequently over large regions. Satellite remote sensing can offer synoptic and systematic information on vegetation conditions useful in environmental monitoring. However, fine-scaled erosive features, such as small deflation patches, may not be easily identifiable in moderate resolution imagery (10-30 m). Here the integration of Unoccupied Aerial Vehicle (UAV), Sentinel-2, and field data is examined to bridge the gap between ground-based and spaceborne monitoring. High resolution (< 5 cm) UAV-based land cover maps are produced for six sites, achieving high overall accuracy (> 90%) compared to ground measurements. These data are upscaled via a regression model estimating bare soil cover, yielding good results ($R^2 = 0.81$). Using land-monitoring data from the Icelandic National monitoring program GróLind, erosion severity classes are defined and mapped. This study highlights the potential of multiscale remote sensing for estimating sub-pixel landscape information and improving automated soil erosion mapping.

Keyword: Soil erosion, Unoccupied aerial vehicle, Machine learning, Satellite, Vegetation Indices, Multi-scale

YFIRLIT

Uppskölun fjarkönnunargagna frá flygildum til að fylgjast með jarðvegsrofi á norð austur hálendi Íslands. Jarðvegsrof er eitt af stóru umhverfisvandamálum á Íslandi í dag og hefur hraði og alvarleiki jarðvegsrofs sterk tengsl við gróðurþekju. Núverandi aðferðir við kortlagningu og vöktun jarðvegsrofs á Íslandi eru kostnaðarsamar og erfitt er að beita þeim reglulega á stór svæði. Fjarkönnun með gervitunglamyndum getur veitt heildstæða mynd af ástandi gróðurs sem getur nýst við umhverfisvöktun. Hins vegar getur verið erfitt að greina smágerðar rofmyndir, eins og rofdíla, í venjulegri upplausn gervitunglamynda (10-30 m). Í þessari rannsókn er samþætt notkun flygilda (e. Unoccupied Aerial Vehicle, UAV), Sentinel-2 gervitunglagagna og vettvangsgagna skoðuð sem möguleiki til að brúa bilið á milli athugana á jörðu niðri og gervitunglaathugana. Landþekja sex svæða var kortlögð í hárri upplausn (< 5 cm) með flygildi og gáfu niðurstöðurnar góða heildarnákvæmni (e. accuracy, >90%) samanborið við vettvangsmælingar. Þessar upplýsingar voru síðan skalaðar upp fyrir gervitunglagögn með aðhvarfslíkani (e. regression model) til að meta þekju óvarins jarðvegs, með góðum árangri (R² = 0.81). Með notkun gagna úr landvöktunarkerfinu GróLind voru rofflokkar svo skilgreindir og kortlagðir út frá þekju óvarins jarðvegs. Rannsóknin sýnir fram á möguleikann á notkun fjölkvarða-fjarkönnunar til að meta landupplýsingar út frá myndeiningum og að sjálfvirknivæða kortlagningu jarðvegsrofs.

INTRODUCTION

Soil erosion is a geomorphic process through which soil particles (sediments, soil aggregates, and organic matter) are entrained and transported away from their primary location (Poesen 2018). Through intense erosion, soils become less fertile as nutrients are removed (Arnalds et al. 2001). Natural erosive processes such as rain, wind, and gravity, as well as biological processes including trampling and burrowing by wildlife, are typical in most landscapes (Poesen 2018). Anthropogenically induced changes in land use and climate, however, can amplify and accelerate erosion beyond the capability of an ecosystem to generate new soil, causing rapid landscape degradation (Borrelli et al. 2021, Poesen 2018).

Vegetation cover has a strong influence on the rate and severity of soil erosion (Durán Zuazo et al. 2008, Gyssels et al. 2005). Vegetation can shield erosion-prone soil from wind and precipitation and provide support against gravity on slopes, limiting soil loss (Tang et al. 2021). Vegetation composition, structure, and coverage are changing in many high latitude regions due to climate change and other anthropogenic pressures. The exact nature of these changes, however, and their impact on soil erosion is complex and not well understood (Myers-Smith et al. 2020, Streeter & Cutler 2020). Monitoring must be improved to better understand the impact of vegetation cover change on soil erosion and to effectively target restoration efforts, such as revegetation, toward areas showing early signs of erosion.

Regions of Iceland have experienced rapid and severe landscape degradation since human settlement in the 9th century, including dramatic loss in vegetation and increase in soil erosion (Arnalds 2015, Dugmore et al. 2009, Greipsson 2012, Ólafsdóttir et al. 2001). This is particularly true for the Highland region, which encompasses remote wilderness areas above the potential treeline (approx. 200-400 m a.s.l, Boulanger-Lapointe et al. 2022) and where sub-alpine tundra vegetation is dominant (Thórhallsdóttir 1997). Grazing pressure increased dramatically in the Highland with animal husbandry

accompanying human settlement, ~1,100 years ago (McGovern et al. 2007). The Highland is most sensitive to this change, due to the short growing season and disturbance from glacial and volcanic activity (Arnalds et al. 2023, Dugmore et al. 2009). Disturbed vegetation in this region is slow to recover, leaving soil exposed to further disturbance. The soils found in much of the Highland tend to lack strong cohesive properties and are easily entrained by frequent, strong winds (Arnalds 2015). The result is the poor land conditions seen in many parts of Iceland today, with over 39% of the country's total area considered to be eroded as of 2001 (Arnalds et al. 2001, 2023).

Currently, the main source of geospatial erosion data for Iceland comes from a series of maps produced between 1991 and 1997 by the Agricultural Research Institute (ARI) and the Soil Conservation Service of Iceland (SCSI; now Land and Forest Iceland), using field observations and manual interpretation of Landsat 5 imagery. The project produced coarse resolution products that categorized erosion severity into 6 classes according to the areal coverage of landscape features indicative of active erosive processes, for example Rofabards (escarpments), erosion spots, and sand encroachment (Arnalds et al. 2001, Arnalds 2015). These maps provide critical quantification of land conditions on a wide scale. However, in the 27 years since these maps were produced, it is likely that land conditions have changed in many regions. This includes both the progression and regression of soil erosion. Thus, the ability to accurately examine and analyze current land conditions using these maps is limited (Arnalds et al. 2023).

Satellite imagery and machine learning are important tools that have improved the accuracy and efficiency of many monitoring and mapping tasks, including those related to soil erosion (Sepuru & Dube 2018). Such tools have been applied to regions of Iceland in previous studies. Fernández et al. 2022 highlighted the potential of remote sensing for this application, using Sentinel-2 imagery alongside topographic data to predict erosion risk from field observations

of erosion severity provided by the SCSI. While the results show good accuracy, nuanced information is lost in the broad 6-point classification scheme, and physical attributes important to management, such as vegetation cover, cannot be interpreted from the results.

The Normalized Vegetation Index (NDVI) is commonly used as a proxy for vegetation cover. NDVI takes advantage of the divergent spectral response of green vegetation in the red and near infrared (NIR) portions of the electromagnetic spectrum. In simple terms, when used as a proxy for vegetation cover, high NDVI values are interpreted as indicating dense, healthy green vegetation. Low NDVI values are interpreted as indicating a lack of vegetation and therefore the relative dominance of bare surface cover (Hurcom & Harrison 1998, Xiao & Moody 2005).

While NDVI can be well correlated with vegetation cover in some settings, this is not always the case, as NDVI values can be influenced by factors such as topography and vegetation phenology (Ayalew et al. 2020, Laidler et al. 2008). Changing climate in the Arctic, which drives change in vegetation composition, further breaks down this relationship. In particular, the increase in tundra shrub cover is thought to inflate the near infrared (NIR) portion of the spectral profile and therefore the NDVI signal (Juszak et al. 2014). This means that, as shrubs encroach into an area experiencing erosion, loss of vegetation cover may be masked by their higher NDVI value (Kodl et al. 2024). Other vegetation indices (VIs), such as the Normalized Difference Red-Edge 1 (NDRE1), have shown promise in determining vegetation cover. Previous studies suggest that these VIs should be considered in addition to NDVI (Andreatta et al. 2022, Riihimäki et al. 2019). Furthermore, other VIs show better sensitivity than NDVI for tundra species, especially VIs using red-edge (RE) bands (Buchhorn et al. 2013, Liu et al. 2017).

Arctic tundra landscapes display a high degree of spatial heterogeneity, meaning that in moderate and coarse resolution satellite imagery various landscape features can occupy a single pixel (Virtanen & Ek 2014). As the spectral information of a pixel is an aggregate from the features within it, it can be difficult to disentangle the role that characteristics (e.g., areal coverage & configuration) of individual features have on spectral response from traditional field observations. Uncrewed aerial vehicles (UAVs) can produce very high-resolution imagery and continue to become more accessible for research and management communities. There are various ways in which UAV and satellite data can be used synergistically. One approach is the calibration of satellite data or models applied on satellite data using UAV data. This approach can be used as a form of data upscaling to expand on information initially derived from the UAV data and to offer an alternative to traditional field observations (Alvarez-Vanhard et al. 2021).

UAV data upscaling has been shown as an effective method for model calibration in fractional land cover problems relating to tundra and similarly heterogeneous landscapes (Bergamo et al. 2023, Riihimäki et al. 2019). By applying machine learning at multiple scales, linked through spatial aggregation, the dominance of sub-pixel physical characteristics can be estimated. Examples of the use of UAV to upscale previous applications include mapping fractional coverage of invasive shrub species in northern Estonia (Bergamo et al. 2023) and forage lichen in northern Canada (Fraser et al. 2022).

It remains difficult to capture fine variation in soil erosion across large and remote regions like the Highland of Iceland. Field-based monitoring is labor intensive and coverage limited. Satellite imagery offers broad coverage, but sub-pixel heterogeneity is obscured. UAV imagery provides the potential to bridge the gap between these two scales by linking fine resolution information to satellite data. The aim of this study is to examine the integration of UAV and satellite data through upscaling, as a means for estimating bare soil and rock cover (hereafter refer to as bare soil cover) for soil erosion monitoring. This is accomplished by using UAV scale image classification to train a satellite-based model that estimates bare soil cover. The relationship between bare soil cover and erosion severity in existing, field based, land monitoring data is used to classify erosion severity from the satellite-scale model. The goal of this approach is to provide a framework for improved and automated mapping of soil erosion across the Highland of Iceland.

MATERIALS AND METHODS

Study site

The study was conducted at six sites located in northeastern Iceland (Figure 1). Sites were randomly chosen in the Múlaþing and Norðurþing areas of the Highland, above 400 m elevation (Arnalds et al. 2023). All sites are located within open sheep grazing commons (Arnalds & Barkarson 2003). The Möðrudalur weather station nearby shows a mean annual temperature of 1.30 °C and mean monthly wind speed of 0.97 m s⁻¹ from 2007 to 2023 (Icelandic Meteorological Office 2024). Vegetation types

in the region are a mix of heath, grasslands, moss heaths and wetlands (Kardjilov et al. 2006). The UAV survey sites encompass a range of erosion severity, from fully vegetated to severely eroded areas (Arnalds et al. 2001). Soils in the regions are Andosolic and Vitrisolic, the former characterized by high carbon content, low bulk density and high water storage capacity, whereas the latter is characterized by low organic material and clay content, with low water storage capacity. Andosols support some of the most densely vegetated regions of Iceland, whereas Vitrisols support little biological activity, meaning that soils of this type are exposed to transport by wind and water (Arnalds 2015, Arnalds & Oskarsson 2009).

Data and pre-processing UAV and Sentinel-2 Imagery

In July 2023, imagery was collected along six 1.4 - 3.1 km transects in eastern Iceland. Transects were used to capture as much within-

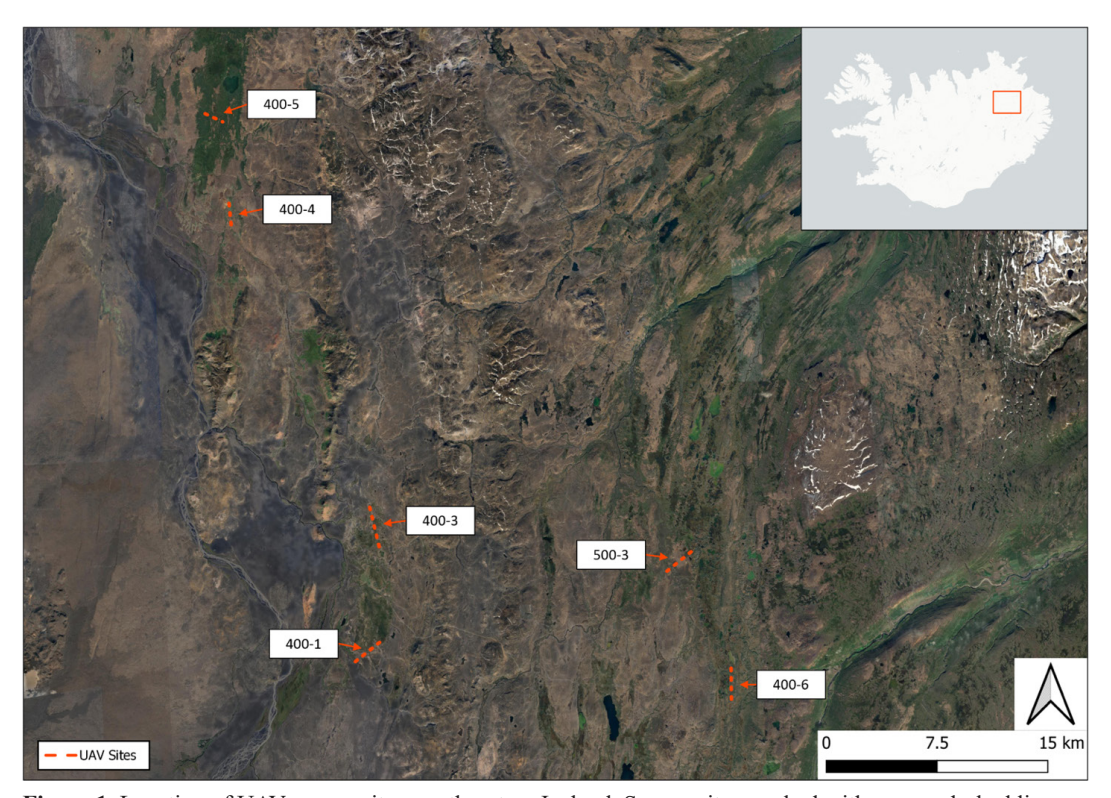


Figure 1. Location of UAV survey sites, northeastern Iceland. Survey sites marked with orange dashed lines.

site variance while maintaining consistent elevation for each site to limit variation in environmental factors. The RGB sensor onboard a DJI Mavic 3T quadcopter UAV was used, with the red band at 650 nm (±16 nm) the green at 560 nm (± 16 nm) and the blue at 450 (± 16 nm). The UAV was flown at approximately 80 m above ground level. Images were set to capture 80% front overlap. The width of each transect was approximately 60 m. Best attempts were made to conduct all flights around solar noon, however, due to weather, flight times varied by up to 5 hours. Differences in illumination, however, were minimal due to the long daylight hours during this time of year.

The UAV data were processed in Agisoft Metashape version 2.1.0. Photogrammetric applied processing was following recommended steps from the software developers (Agisoft LLC., St. Petersburg, Russia). Images containing excessive motion blur were removed prior to processing. Georeferencing was based on the GPS unit and internal measurement unit onboard the UAV, producing an estimated horizontal positioning error of ~3 m. This process produced a single orthomosaic for each of the six transects with spatial resolutions of 4-5 cm.

Sentinel-2 data for the region was acquired in 16-bit from the Sentinel-2 Global Mosaic Service, using the Advanced Temporal Mosaic tool. The temporal range was set between 31 July 2023 and 31 August 2023, returning level 2A imagery from 9 August and 29 August 2023. The SEN2COR atmospheric correction method and ESA cloud mask options were used (Main-Knorn et al. 2017, Sentinel-2 Global Mosaic Service 2014).

Vegetation indices

To provide more information to the UAVscale model and improve vegetation and soil separability, two RGB VIs were calculated using the *terra* package for R v4.2.2 (Hijmans 2023, R Core Team 2022). The two VIs, VIgreen and EXGR, were selected based on their ability to effectively separate bare soil and vegetation, demonstrated in a previous study

(Vieira & Rodrigues 2021). To calculate these VIs the RGB data was first normalized with a two-step process using equations 1 and 2, where R, G, and B are the original values, R_{max} , G_{max} , and B_{max} are the maximum of the 8-bit channels (255), and r, g, and b are the final normalized spectral components (Guijarro et al. 2011, Marcial-Pablo et al. 2019, Vieira & Rodrigues 2021). The VIs were then calculated using equations presented in Table 1.

(1)
$$R_n = \frac{R}{R_{max}} G_n = \frac{G}{G_{max}} B_n = \frac{B}{B_{max}}$$

(2)
$$r = \frac{R_n}{R_n + G_n + B_n} g = \frac{G_n}{R_n + G_n + B_n} b = \frac{B_n}{R_n + G_n + B_n}$$

Four VIs were calculated with the Sentinel-2 data to be used in the satellite scale model. As with the UAV VIs, these indices are meant to emphasize vegetation and to improve bare soil detection. GCI, MSAVI2 and NDVI were selected based on their performance when previously applied to identify overgrazing hotspots (Table 2, Harmse et al. 2022). Additionally, NDRE1 was selected based on its potential shown in a previous study to identify bare soil and performance in regions of low vegetation cover (Table 2, Andreatta et al. 2022). Sentinel-2 bands 5 and 6 are 20 m resolution and therefore were resampled, using a bilinear approach, to match the 10 m resolution of the remaining bands used.

Table 1. Description of RGB vegetation indices used for UAV scale classification.

Name	Equation	References
Vegetation Index Green	$VIgreen = \frac{g - r}{g + r}$	(Gitelson et al. 2002)
Excess Green minus Excess Red	EXGR = (2g - r - b) - (1.4r - g)	(Meyer & Neto 2008)

In-situ bare soil cover measurements

To compare bare soil cover estimates based on the UAV classification to those that would be recorded by a field technician, ten randomly selected points along each transect were overlaid with a 50 cm-by 50 cm quadrat, prior to each UAV flight. An image of each quadrat placement

Name	Formula	Bands	References
Green	$GCI = (\frac{NIR}{Green}) - 1$	8,3	(Gitelson et
Chlorophyll Index	orech.		al. 2005)
Modified Soil	$MSAVI2 = \frac{2 * NIR + 1\sqrt{(2 * NIR + 1)^2 - 8(NIR - Red)}}{2}$	8,4	(Qi et al.
Adjusted	$MSAV1Z = {2}$		1994)
Vegetation			
Index 2			
Normalized	$NDVI = \frac{(NIR - Red)}{(NIR + Red)}$	8,4	(Tucker
Difference	(NIR + Red)		1979)
Vegetation			
Index			
Normalized	$NDRE1 = \frac{(RE_{740} - RE_{705})}{(RE_{740} + RE_{745})}$	6,5	(Gitelson &
Difference Red	$(RE_{740} + RE_{705})$		Merzlyak
Edge 1			1994)

Table 2. Description of Sentinel 2 vegetation indices used for the satellite scale regression model.

was taken at waist height (~105 cm) with a digital camera (Figure 2), and the percent bare soil within the quadrat was recorded. For later identification of the exact quadrat placements in the UAV imagery, a flag was placed at the center of each quadrat, and the location was recorded with a Garmin Etrex 10 handheld GPS unit with an average positional error of ~5 m.

Each quadrat placement was identified in the orthomosaics, and a 50 cm-by 50 cm polygon was drawn around the flag, using the corresponding field photograph to inform polygon delineation. To arrive at a classification-based bare soil cover value that could be directly compared to the field observation, the percent of bare soil cover was calculated for each polygon, using the zonal histogram tool in QGIS v3.28 (QGIS Development Team 2009). The classification-based estimate was evaluated using Root Mean Square Error (RMSE).

Soil erosion data

GróLind is the most extensive and up to date land monitoring initiative from the Soil Conservation Service of Iceland (now Land and Forest Iceland). Each monitoring site consists of a 50 x 50 m plot. Approximately 200 sites are visited annually, resulting in a five-year revisit time for each site. At these sites variables relating to ecological status are recorded, including vegetation height and cover, soil depth, soil type, and erosion rating (Marteinsdóttir et al. 2021). The erosion rating is based on the system outlined by Arnalds et al. (2001) which considers erosional features, typically defined by areas of exposed soil, such as sand encroachment, erosion spots, and Rofabards, as well as general vegetation cover. This system uses qualitative visual observations classified on a five-point scale, with 0 representing no erosion and 5 representing extreme erosion. Vegetation cover is also estimated based on visual observation on a scale of 1-5 (i.e. 1: 91-100%; 2: 67-90%; 3: 34-66%; 4: 11-33%; 5: 0-10%). For our analysis, we considered vegetation cover as a proxy of bare soil cover, since the total cover at one site is only made of vegetation and bare soil, including exposed rocks (e.g. a vegetation cover rating of 1 means both high vegetation cover and low bare ground cover). We used data

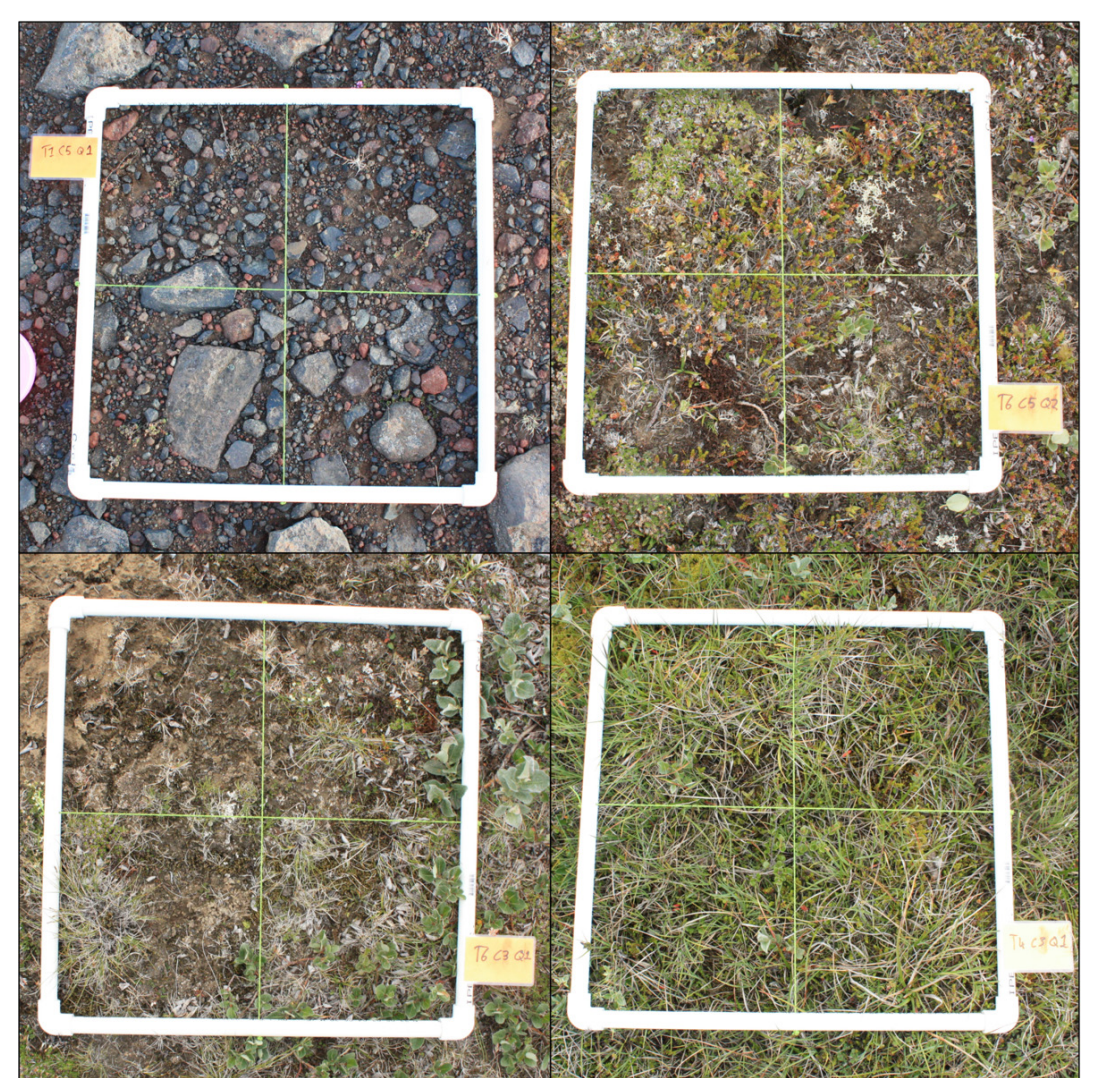


Figure 2. Example of quadrat placements used for field validation of the UAV-scale classification.

from sites visited in 2019 (n=79) to examine the relationship between erosion severity and bare soil cover (Figure 3d).

UAV and satellite data processing UAV-scale classification

For the UAV-scale classification training and validation, data were generated for 5 class types: bare soil (dark), bare soil (light), green vegetation, non-green vegetation (e.g. white lichen, flowers), and water (Figure S1). The goal of using these classes rather than a binary bare soil presence-absence scheme was to reduce error by providing narrow classes with less variation in spectral signature. Along each transect ten 50 x 50 cm polygons were manually delineated for each class, in QGIS (QGIS Development Team 2009), resulting in 50 polygons per transect. The location of the polygons was determined by examining the RGB orthomosaics and selecting areas of homogeneous, class representative cover.

The two VIs, of the normalized RGB bands and the raw orthomosaic RGB bands, were used

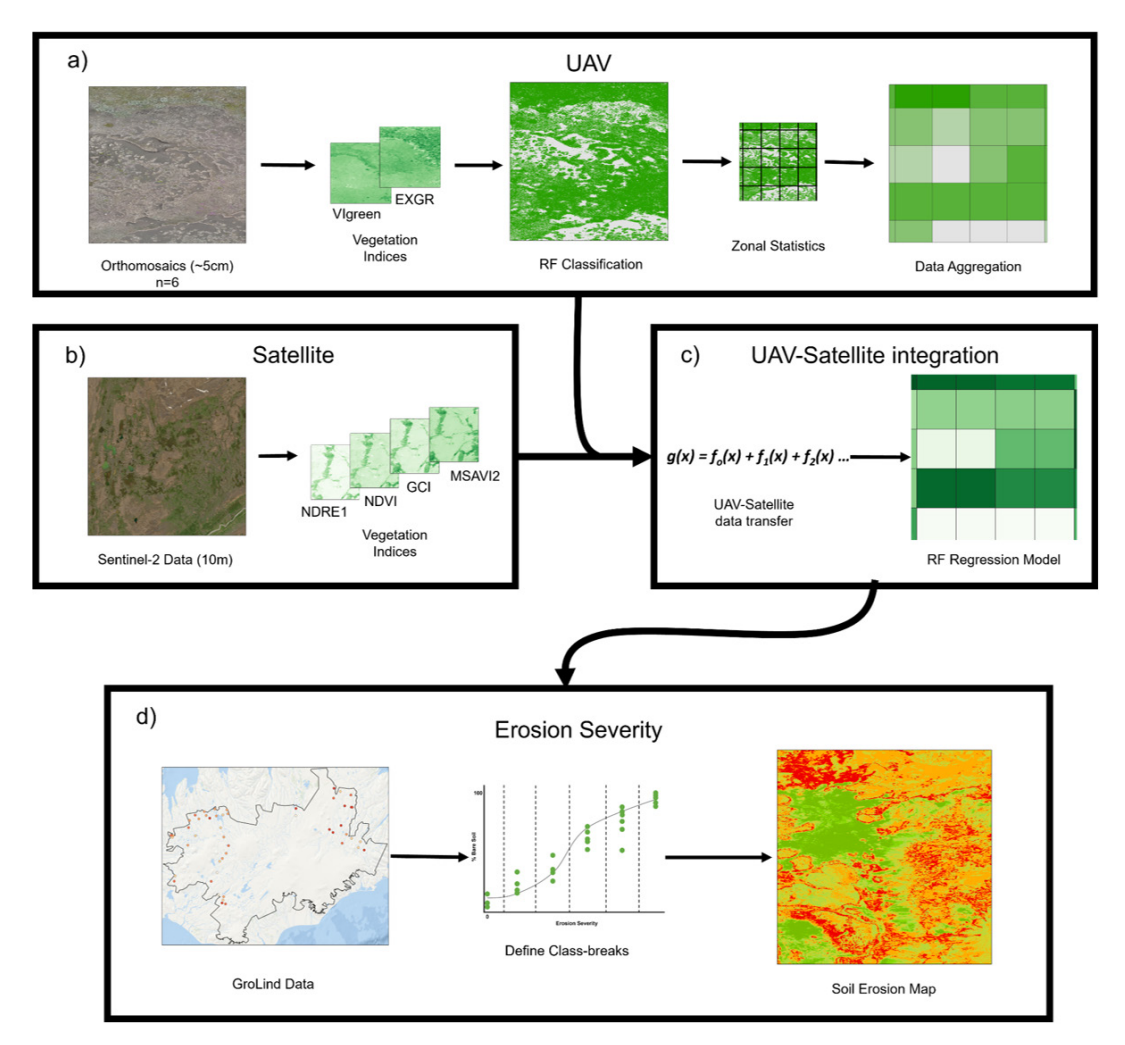


Figure 3. Workflow for UAV data upscaling and erosion severity mapping. a) UAV data treatment after preprocessing, b) Sentinel-2 satellite data treatment, c) UAV and Sentinel-2 satellite data integration, d) integration of GróLind data for erosion severity mapping.

as predictive variables. Each pixel within the polygons (~360 per polygon) was sampled to extract values for these variables. This provided approximately 18,000 sampled points per transect. These data were split randomly into training (70%) and validation (30%) sets, using a stratified approach to ensure an equal number of training and validation points between the five classes.

A random forest classification model was implemented using the *caret* and *randomForest* packages in R (Kuhn 2008, Liaw & Wiener

2002). Random forest was chosen based on the accuracy of the model for classifying land cover from RGB UAV imagery that was demonstrated in previous studies (Bergamo et al. 2023, Fraser et al. 2022). An individual model was fit for each transect to improve site-specific accuracy due to the previously-mentioned variation in illumination conditions (Kodl et al. 2024). Since an independent testing dataset was not available, a 10-fold cross validation, which provides good prediction estimates (Wadoux et al. 2021), was used to test model accuracy. The number of

variables to randomly sample at each split, a parameter known as mtry, was optimized using a grid search, testing values between 1 and 8. The number of trees was set to a constant of 500. A confusion matrix was produced for each site using the validation data. Accuracy and Kappa values were used to assess model performance. The model with optimal parameterization for each site was applied to a stack of raster layers containing the eight variables.

Upscaling

To upscale the UAV-scale classification, a within-pixel coverage method was used to find percent bare soil (Bergamo et al. 2023, Riihimäki et al. 2019). A grid was generated directly from the Sentinel-2 data to match the 10-m spatial resolution. Segments of this grid were clipped to match the extent of each transect. The zonal histogram tool in QGIS was used to compute the number of pixels in the UAV-scale classification assigned to each of the five classes, within each grid cell. The two bare soil classes were merged and compared to the occurrence of the remaining classes within each grid cell to determine the percent bare soil coverage (0-100).

Satellite-scale regression model

A point was placed at the center of each grid cell produced in the upscaling process. The calculated percent bare soil for each cell was then transferred to the corresponding point. The values from each of the Sentinel-2 variables. bands 2-8, and the four VIs were sampled at each point. This produced 18,287 data points. These data were split into training (70%) and validation (30%) sets.

A random forest regression model was implemented on the training data using the caret and randomForest packages in R (Kuhn 2008, Liaw & Wiener 2002). Random forest was chosen based on its accuracy in upscaling applications presented in previous studies (Fraser et al. 2022). A model fitting procedure, like that used for the UAV-scale classification model, was implemented with 10-fold cross validation. The mtry parameter was optimized using a grid search with values between 1 and 11. The number of trees was set to a constant of 500. The best model was chosen based on RMSE and R². The best model was run on the validation set. and the RMSE and R² were calculated to assess the model's predictive performance. The final model was applied to a stack of raster layers containing the 11 variables.

Erosion severity

The GróLind data were subset to contain only points within the Highland region (above 400m elevation), leaving 76 sites collected in 2019. A Pearson correlation test was run to establish if there is a significant relationship between the erosion severity and bare soil cover data that was collected in the field by the GróLind program. The results indicated a strong positive and significant relationship (r = 0.82, p < 0.005). A linear regression was fit to estimate erosion severity from bare soil cover in this dataset. The satellite-scale continuous bare soil cover model was then reclassified to the five-point bare soil cover ranking used by the GróLind program, and the linear regression was applied to these data to estimate soil erosion severity for each pixel in the satellite images. Non-whole values of erosion severity were reclassified to the nearest whole number to fit the five-point GróLind classification scheme (e.g. $1.5 \rightarrow 2$).

RESULTS

UAV-scale classification

The random forest classifier produced an overall accuracy of 96.6% across all six sites with a Kappa of 0.95 and RMSE of 15.36% (Table 3; see Table S1 for confusion matrix and F-1 scores). The best results were achieved at site 400-5, with an accuracy of 98.6% and Kappa of 0.98. The lowest results were achieved at site 400-3 with an accuracy of 92.2%, a Kappa of 0.90, and RMSE of 40.17%. Aside from site 400-3, all sites achieved accuracy greater than 95%, Kappa scores greater than 0.94, and RMSE less than 9%.

Table 3. Summary of the accuracy results for UAV-scale classification at each site and overall. accuracy and Kappa based on cross validation, RMSE based on quadrat fractional coverage. Due to human error in the field the quadrat points for two sites (400-1, 400-5) fell outside of the UAV imagery as a result the quadrat based RMSE values for those two sites could not be calculated.

Site	Classification metrics		Field data metric	
	Accuracy (%)	Kappa	RMSE (%)	
Overall	96.6	0.95	15.36	
400-1	97.4	0.97	6.67	
400-3	92.2	0.90	40.17	
400-4	96.6	0.94	-	
400-5	98.6	0.98	-	
500-3	97.8	0.97	8.78	
500-6	97.0	0.96	5.76	

Upscaling UAV data

Relatively large erosional features, where continuous areas of bare soil are exposed, are well represented in both the UAV classification and the aggregated data (Figure 4). Away from the center of these features, exposed soil becomes fragmented and appears in smaller patches as vegetation cover increases. This pattern is distinct in the UAV-scale classification

results. Due to the aggregation inherent in the upscaling process, however, this pattern is obscured when the pixel size becomes much larger than individual erosional patches. While the aggregated data tend to show the pattern of increased vegetation with distance away from erosional features, the distribution of exposed soil within a cell is lost (Figure 4).

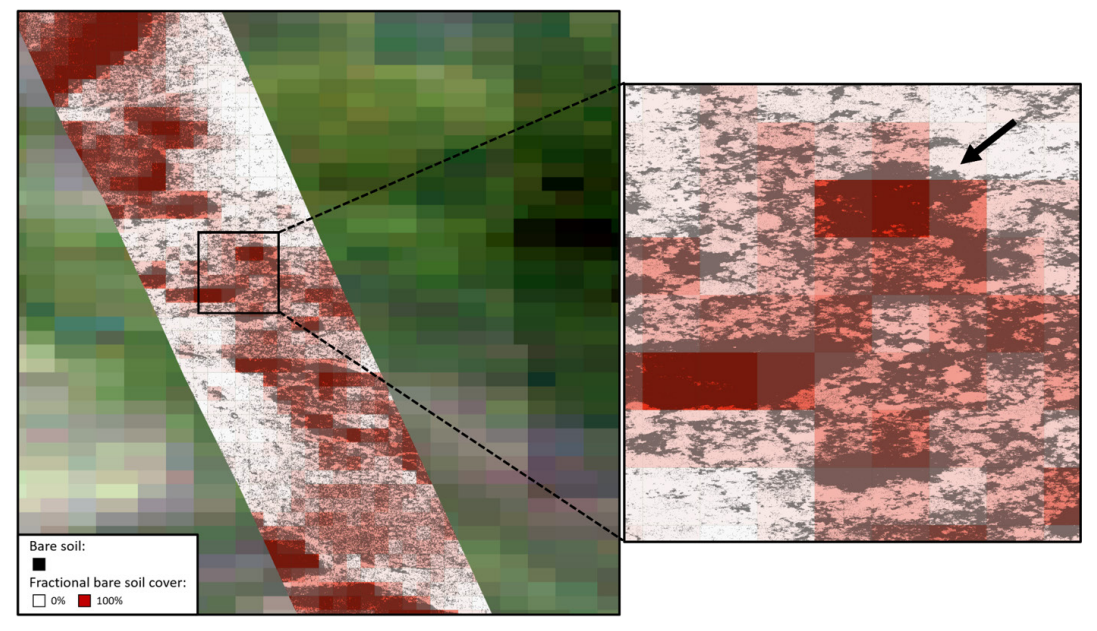


Figure 4. UAV-scale classification of bare soil shown in black (presence of bare soil), overlain with fractional bare soil coverage produced from aggregation during the upscaling process, site 400-3. Black arrow on the left panel shows an example of an erosional feature edge being obscured due to aggregation.

Satellite regression and erosion severity

The satellite-scale percent bare soil cover regression model produced an R² of 0.814 for all sites (Figure 5a). The site-specific results show a wide range of R² values. Site 400-1 (Figure 5b) produced the lowest R² (0.403), showing a large number of points estimated to have a greater bare soil and cover than classified in the

UAV data. Site 500-3 produced the highest R² (0.924). The final bare soil cover map (Figure 6a) displays upscaled results, allowing for visual interpretation as well as identification of gaps and errors. The soil erosion rating map (Figure 6b) presents those same results using the SCSI classification scheme.

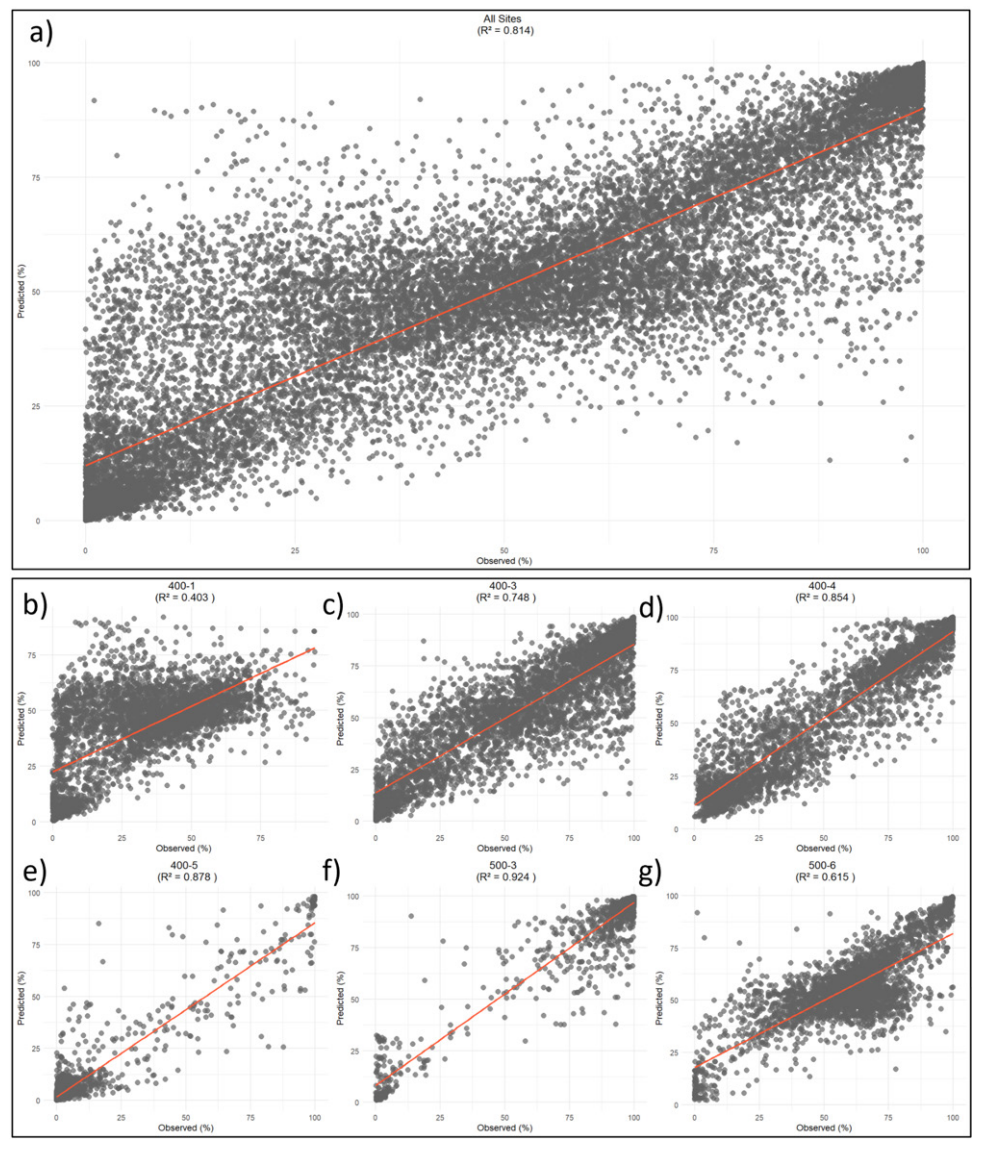


Figure 5. Scatter plots showing the percent bare soil coverage from the satellite-scale regression model (predicted) compared to the aggregated UAV-scale classification (observed), best fit line shown in orange. Top (a) panel shows the results for all six sites overall. Bottom (b-g) panel shows the results at each site.

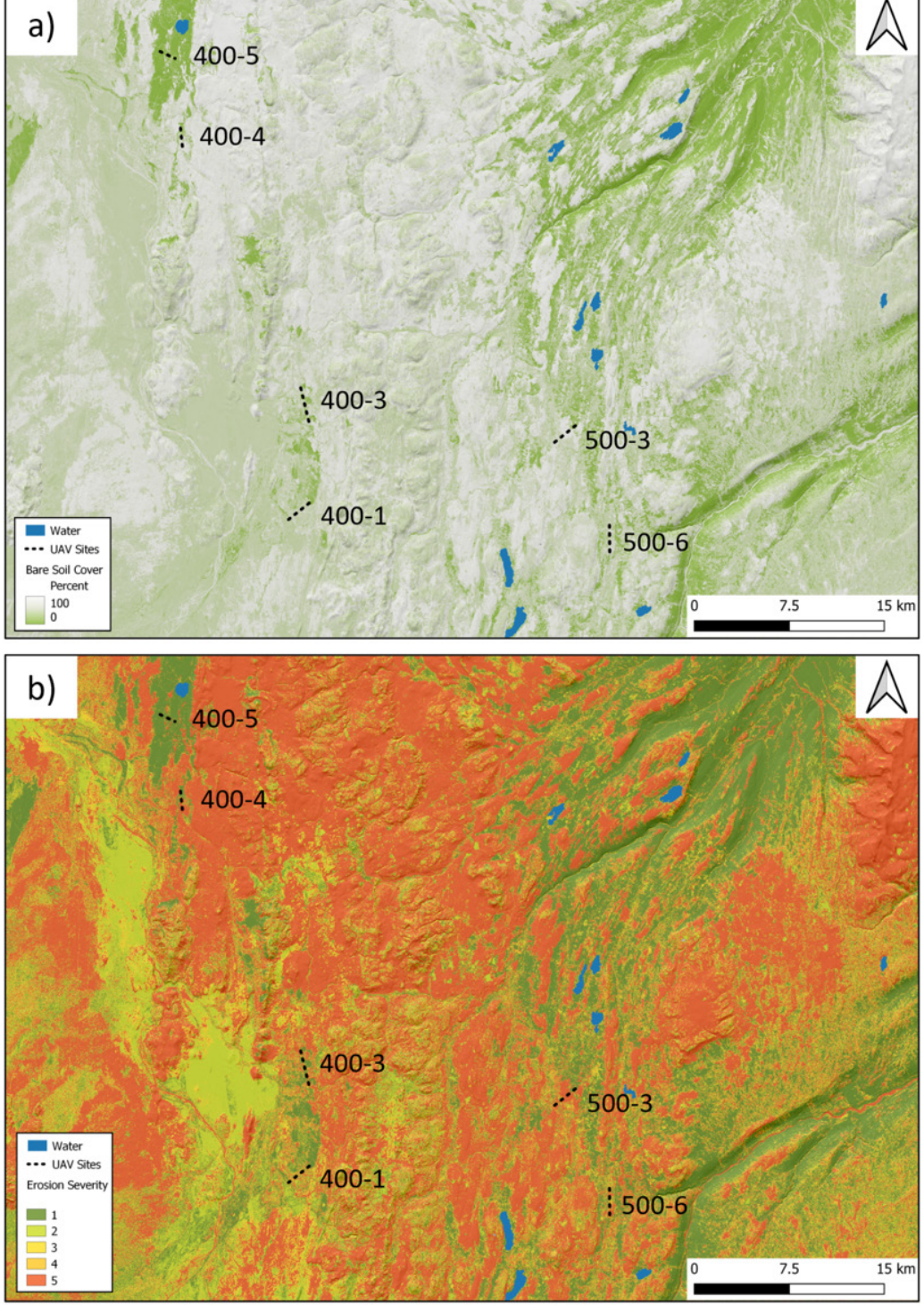


Figure 6. a) Percent bare soil cover map from upscaled UAV data, b) erosion severity map derived from the upscaled bare soil cover ranked using the GróLind erosion severity classes.

DISCUSSION

This study illustrates the potential of integrating UAV and satellite data to extract physical parameters, in this case vegetation cover, for mapping and monitoring soil erosion in tundra environments. The methods presented here show that UAV data upscaling with a random forest regression model can provide continuous estimates of percent bare soil cover at the satellite pixel scale. The use of UAV data in this way could provide a cost-effective alternative to on-foot field measurements and produce high quality training data for semi-automated mapping from satellite imagery. Parameters upscaled from UAV data could be integrated with existing soil erosion data generated by the ongoing GróLind program to expand the scope beyond measured locations (Bergamo et al. 2023).

UAV-scale classification

The UAV-scale random forest classifications based on RGB VIs were able to separate bare soil and vegetation with accuracies comparable to multispectral UAV based classifications (Furukawa et al. 2021). The use of multiple VI's and a five-class scheme builds upon results of previous studies that implemented a binary scheme on RGB digital number data alone (Riihimäki et al. 2019). Due to the singleimage width of the orthomosaics used in this study, digital elevation models (DEMs) could not be generated for the UAV sites. The use of such DEMs in the UAV-scale classification could further improve accuracy by generating point clouds that can be used to assess textural information (Bergamo et al. 2022).

The site-specific classification accuracy shows low variation, with a range of 6.4% and 0.08 in accuracy and Kappa measures among sites, respectively. Other studies that have implemented RGB UAV data for vegetation classification tasks show similar results across a range of environmental settings (Bergamo et al. 2023, Furukawa et al. 2021, Riihimäki et al. 2019). The low variation in accuracy between sites may be due in part to the site-specific model approach taken here. While fitting an individual model for each site is more time consuming, compared to fitting a single model across all sites, it likely limits the error induced by variations in illumination and weather conditions (Furukawa et al. 2021, Wang et al. 2023). This is an important consideration for implementing these methods across a broader area and in regions where weather can change dramatically over short periods, such as in northeastern Iceland.

Upscaling and satellite scale mapping

The satellite-scale random forest regression model shows high overall agreement (R² = 0.814) with the UAV based bare soil cover data (Figure 4 & 5a). These results highlight the usefulness of these models for estimating bare soil cover across a Sentinel-2 pixel. Previous studies have illustrated the power of random forest regression for estimating fractional cover of invasive plant species from satellite data, producing accuracy like that shown here (Kattenborn et al. 2019, Shiferaw et al. 2019). While random forest regression appears to be a robust model for UAV upscaling, based on these results and those of previous studies, various models should be examined through more-exhaustive performance measures and for variables beyond those related to vegetation (Fraser et al. 2022, Kattenborn et al. 2019)

The site-specific regression accuracies show large variations, with R² values much lower than the overall value. The lowest R² (0.403) was produced at site 400-1 (Figure 5b). Site 400-1 is characterized by a consistent pattern of many small bare soil patches (5 - 20 cm diameter) and a high degree of non-green vegetation cover (i.e. areas covered by white lichen or flowering plants), which are common in Iceland. The VI's used for the satellite-scale regression model largely rely on the NIR and red bands, as do most widely used VI's. The spectral signature produced by non-green vegetation at these wavelengths is not as easily distinguished from bare soil as is green vegetation (French et al. 2008). This is likely why the model predicts higher bare soil cover at site 400-1 than is shown in the UAV data. The inclusion of shortwave infrared (SWIR) information or indices may improve the performance of the model for areas dominated by non-green vegetation, but that would come at the expense of spatial resolution. Green and non-green vegetation show increased separability in the 2200 nm range, thus the use of Sentinel-2 band 12 (2190 nm) could be used in future applications where higher spatial accuracy is not a prerequisite (Amin et al. 2021). Despite the lack of NIR and SWIR information in the UAV data, the classification achieved good results in separating bare soil and non-green vegetation for site 400-1 (Table 3). This is likely due to the high resolution of the UAV data, suggesting that increased resolution may be able to improve separability of spectrally similar cover types. Therefore, higher resolution multispectral satellite data, for example PlanteScope (3 m), may better detect non-green vegetation.

Finally, the UAV sites largely missed regions of very dark sands and gravel, like those near site 400-4 and 400-5 (Figure 1). In the bare soil cover map produced by the upscaling process (Figure 6a), regions with this composition appear to have higher vegetation cover than expected. As a result, the erosion severity assigned to these areas tends to be lower than anticipated. While the sampling design was meant to capture changes in relation to the elevational gradient, a different sampling strategy would be needed to capture the spectral signature of these distinct areas.

Future work

While the fraction of bare soil to vegetation cover over a given area is strongly related in many areas to soil erosion, it is not the sole factor (Zhongming et al. 2010). This study has shown UAV RGB data upscaling to be an effective method for estimating variables related to soil erosion. In addition to improving estimates of bare soil cover, future efforts should investigate additional parameters such as soil moisture, soil surface roughness and phenological stages that may benefit from upscaling. Looking to existing, robust, empirical models, such as the Revised Universal Soil Loss Equation (RUSLE), for parameters that may relate to physical factors

that can be derived and upscaled from UAV data provides a promising path forward (Felix et al. 2023).

Vegetation parameters that relate to soil erosion and that may be explored using methods like those presented here include vegetation type and structure. Erosion severity influences, and is influenced by, the types of vegetation present as well as their distributions over a given area (Jiao et al. 2009, Tsuyuzaki & Titus 1996). For example, previous studies in Iceland successfully upscaled fractional coverage of woody shrub species from UAV data to correct satellite NDVI values to support soil erosion monitoring (Kodl et al. 2024). Others have used upscaled fractional species cover to monitor invasive shrubs (Bergamo et al., 2023).

Producing high resolution DEMs (3-5 cm/ pixel and positional XYZ-accuracy of ca. 1.5 cm; Nota et al. 2022) from UAV site data opens the potential for complex structural variables to be derived, even in environments with low and scattered vegetation. Upscaling of canopy metrics using synthetic aperture radar (SAR) data may be useful in further estimating vegetation structure, due to the various scattering mechanisms associated with SAR and its application in classifying tundra vegetation (Ullmann et al. 2014). SAR can also be used to estimate surface roughness associated with surface sediment properties in regions with little vegetation cover (Gaber et al. 2015). Using high resolution UAV derived DEMs could provide a method for relating SAR backscatter to surface roughness that is associated with small scale erosional features (Ullmann & Stauch 2020).

ACKNOWLEDGEMENTS

The authors would like to express their gratitude to Marteinn Möller for allowing access to their data and support in the field. This study was financially supported by Polar Knowledge Canada, through the Northern Scientific Training Program (NSTP), the University of Victoria, and the University of Iceland. ReSource International provided in-kind support for the field research component.

REFERENCES

Alvarez-Vanhard E, Corpetti T, & Houet T 2021. UAV & satellite synergies for optical remote sensing applications: A literature review. Science of Remote Sensing, 3, 100019.

https://doi.org/10.1016/j.srs.2021.100019

Amin E, Verrelst J, Rivera-Caicedo J P, Pipia L, Ruiz-Verdú A, & Moreno J 2021. Prototyping Sentinel-2 green LAI and brown LAI products for cropland monitoring. Remote Sensing of Environment, 255, 112168.

https://doi.org/10.1016/j.rse.2020.112168

Andreatta D, Gianelle D, Scotton M, & Dalponte M 2022. Estimating grassland vegetation cover with remote sensing: A comparison between Landsat-8, Sentinel-2 and PlanetScope imagery. Ecological Indicators, 141, 109102.

https://doi.org/10.1016/j.ecolind.2022.109102

Arnalds O 2015. The Soils of Iceland. Springer Netherlands.

https://doi.org/10.1007/978-94-017-9621-7

Arnalds O, & Barkarson B H 2003. Soil erosion and land use policy in Iceland in relation to sheep grazing and government subsidies. Environmental Science & Policy, 6(1), 105-113.

https://doi.org/10.1016/S1462-9011(02)00115-6

Arnalds O, Thorarinsdottir E F, Metusalemsson S, Jonsson A, Gretarsson E, & Arnason A 2001. Soil erosion in Iceland. Soil Conservation Service.

Arnalds Ó, Marteinsdóttir B, Brink S H, & Þórsson J 2023. A framework model for current land condition in Iceland. PLOS ONE, 18(7), e0287764.

https://doi.org/10.1371/journal.pone.0287764

Arnalds O, & Óskarsson H 2009. A soil map of Iceland. Nátturufraedingurinn, 78, 107-121.

Ayalew DA, Deumlich D, Šarapatka B, & Doktor D 2020. Quantifying the Sensitivity of NDVI-Based C Factor Estimation and Potential Soil Erosion Prediction using Spaceborne Earth Observation Data. Remote Sensing, 12(7), Article 7.

https://doi.org/10.3390/rs12071136

Bergamo T F, de Lima R S, Kull T, Ward R D, Sepp K, & Villoslada M 2023. From UAV to PlanetScope: Upscaling fractional cover of an invasive species Rosa rugosa. Journal of Environmental Management, 336, 117693. https://doi.org/10.1016/j.jenvman.2023.117693

Borrelli P, Alewell C, Alvarez P, Anache J A A, Baartman J, Ballabio C, Bezak N, Biddoccu M, Cerdà A, Chalise D, Chen S, Chen W, De Girolamo A M, Gessesse G D, Deumlich D, Diodato N, Efthimiou N, Erpul G, Fiener P, ... Panagos P 2021. Soil erosion modelling: A global review and statistical analysis. Science of The Total Environment, 780, 146494.

https://doi.org/10.1016/j.scitotenv.2021.146494

Boulanger-Lapointe N, Ágústsdóttir K, Barrio I C, Defourneaux M, Finnsdóttir R, Jónsdóttir I S, Marteinsdóttir B, Mitchell C, Möller M, Nielsen Ó K, Sigfússon A Þ, Þórisson S G, & Huettmann F 2022. Herbivore species coexistence in changing rangeland ecosystems: First high resolution national open-source and open-access ensemble models for Iceland. Science of The Total Environment, 845, 157140.

https://doi.org/10.1016/j.scitotenv.2022.157140

Buchhorn M, Walker D A, Heim B, Raynolds M K, Epstein H E, & Schwieder M 2013. Ground-Based Hyperspectral Characterization of Alaska Tundra Vegetation along Environmental Gradients. Remote Sensing, 5(8), Article 8.

https://doi.org/10.3390/rs5083971

Dugmore A J, Gisladóttir G, Simpson I A, & Newton A 2009. Conceptual Models of 1200 Years of Icelandic Soil Erosion Reconstructed Using Tephrochronology. Journal of the North Atlantic, 2(1), 1-18.

https://doi.org/10.3721/037.002.0103

Durán Zuazo V H, Rodríguez Pleguezuelo C R, Francia Martínez J R, Cárceles Rodríguez B, Martínez Raya A, & Pérez Galindo P 2008. Harvest intensity of aromatic shrubs vs. soil erosion: An equilibrium for sustainable agriculture (SE Spain). CATENA, 73(1), 107–116.

https://doi.org/10.1016/j.catena.2007.09.006

Felix, F. C., Cândido, B. M., & Moraes, J. F. L. de. 2023. Improving RUSLE predictions through UAV-based soil cover management factor (C) assessments: A novel approach for enhanced erosion analysis in sugarcane fields. Journal of Hydrology, 626, 130229.

https://doi.org/10.1016/j.jhydrol.2023.130229

Fernández D, Adermann E, Pizzolato M, Pechenkin R, & Rodríguez C G 2022. REMOTE MAPPING OF SOIL EROSION RISK IN ICELAND. The International Archives of the Photogrammetry, Remote Sensing and Spatial Information Sciences, XLVIII-4-W1-2022, 135–141. ISPRS WG IV/4, III/10, IV/7, V/1 & ICWG IV/III

Sorres and Open Source Software for Geospatial (FOSS4G) 2022 – Academic Track - 22– 28 August 2022, Florence, Italy.

https://doi.org/10.5194/isprs-archives-XLVIII-4-W1-2022-135-2022

Fraser R H, Pouliot D, & van der Sluijs J 2022.

UAV and High Resolution Satellite Mapping of Forage Lichen (Cladonia spp.) in a Rocky Canadian Shield Landscape. Canadian Journal of Remote Sensing, 48(1), 5–18.

https://doi.org/10.1080/07038992.2021.1908118

Fraser R H, Van der Sluijs J, & Hall R J 2017.

Calibrating Satellite-Based Indices of Burn Severity from UAV-Derived Metrics of a Burned Boreal Forest in NWT, Canada. *Remote Sensing*, 9(3), Article 3.

https://doi.org/10.3390/rs9030279

French A N, Schmugge T J, Ritchie J C, Hsu A, Jacob F, & Ogawa K 2008. Detecting land cover change at the Jornada Experimental Range, New Mexico with ASTER emissivities. *Remote Sensing of Environment*, 112(4), 1730–1748.

https://doi.org/10.1016/j.rse.2007.08.020

Furukawa F, Laneng L A, Ando H, Yoshimura N, Kaneko M, & Morimoto J 2021. Comparison of RGB and Multispectral Unmanned Aerial Vehicle for Monitoring Vegetation Coverage Changes on a Landslide Area. *Drones*, 5(3), Article 3.

https://doi.org/10.3390/drones5030097

Gaber A, Soliman F, Koch M, & El-Baz F 2015. Using full-polarimetric SAR data to characterize the surface sediments in desert areas: A case study in El-Gallaba Plain, Egypt. *Remote Sensing of Environment*, 162, 11–28.

https://doi.org/10.1016/j.rse.2015.01.024

Gitelson AA, Kaufman Y J, Stark R, & Rundquist D 2002. Novel algorithms for remote estimation of vegetation fraction. *Remote Sensing of Environment*, 80(1), 76–87.

https://doi.org/10.1016/S0034-4257(01)00289-9

Gitelson A A, Viña A, Ciganda V, Rundquist D C, & Arkebauer T J 2005. Remote estimation of canopy chlorophyll content in crops. *Geophysical Research Letters*, 32(8).

https://doi.org/10.1029/2005GL022688

Gitelson A, & Merzlyak M N 1994. Quantitative estimation of chlorophyll-a using reflectance spectra: Experiments with autumn chestnut and maple leaves. *Journal of Photochemistry and Photobiology B: Biology*, 22(3), 247–252.

https://doi.org/10.1016/1011-1344(93)06963-4

Greipsson S 2012. Catastrophic soil erosion in Iceland: Impact of long-term climate change, compounded natural disturbances and human driven land-use changes. *CATENA*, *98*, 41–54. https://doi.org/10.1016/j.catena.2012.05.015

Guijarro M, Pajares G, Riomoros I, Herrera P J, Burgos-Artizzu X P, & Ribeiro A 2011. Automatic segmentation of relevant textures in agricultural images. *Computers and Electronics in Agriculture*, 75(1), 75–83.

https://doi.org/10.1016/j.compag.2010.09.013

Gyssels G, Poesen J, Bochet E, & Li Y 2005. Impact of plant roots on the resistance of soils to erosion by water: A review. *Progress in Physical Geography: Earth and Environment*, 29(2), 189–217.

https://doi.org/10.1191/0309133305pp443ra

Harmse C J, Gerber H, & van Niekerk A 2022. Evaluating Several Vegetation Indices Derived from Sentinel-2 Imagery for Quantifying Localized Overgrazing in a Semi-Arid Region of South Africa. *Remote Sensing*, 14(7), Article 7.

https://doi.org/10.3390/rs14071720

Hijmans R J 2023. *terra: Spatial Data Analysis.* https://CRAN.R-project.org/package=terra

Hurcom S J, & Harrison A R 1998. The NDVI and spectral decomposition for semi-arid vegetation abundance estimation. *International Journal of Remote Sensing*, 19(16), 3109–3125.

https://doi.org/10.1080/014311698214217

Icelandic Meteorological Office 2024. Climatological data. Icelandic Meteorological Office. https://en.vedur.is/climatology/data/

Jiao J, Zou H, Jia Y, & Wang N 2009. Research progress on the effects of soil erosion on vegetation. Acta Ecologica Sinica, 29(2), 85–91.

https://doi.org/10.1016/j.chnaes.2009.05.001

Juszak I, Erb A M, Maximov T C, & Schaepman-Strub G 2014. Arctic shrub effects on NDVI, summer albedo and soil shading. *Remote Sensing of Environment*, 153, 79–89.

https://doi.org/10.1016/j.rse.2014.07.021

Kardjilov M I, Gisladottir G, & Gislason S R 2006. Land degradation in northeastern Iceland: Present and past carbon fluxes. Land Degradation & Development, 17(4), 401–417.

https://doi.org/10.1002/ldr.746

Kattenborn T, Lopatin J, Förster M, Braun A C, & Fassnacht F E 2019. UAV data as alternative to field sampling to map woody invasive species based on combined Sentinel-1 and Sentinel-2 data. Remote Sensing of Environment, 227, 61–73. https://doi.org/10.1016/j.rse.2019.03.025

Kodl G, Streeter R, Cutler N, & Bolch T 2024. Arctic tundra shrubification can obscure increasing levels of soil erosion in NDVI assessments of land cover derived from satellite imagery. Remote Sensing of Environment, 301, 113935.

https://doi.org/10.1016/j.rse.2023.113935

Kuhn M 2008. Building Predictive Models in R Using the caret Package. Journal of Statistical Software, 28(5), 1-26.

https://doi.org/10.18637/jss.v028.i05

- Laidler G J, Treitz P M, & Atkinson D M 2008. Remote Sensing of Arctic Vegetation: Relations between the NDVI, Spatial Resolution and Vegetation Cover on Boothia Peninsula, Nunavut. Arctic, 61(1), 1–13.
- Liaw A, & Wiener M 2002. Classification and Regression by randomForest. R News, 2(3), 18–22.
- Liu N, Budkewitsch P, & Treitz P 2017. Examining spectral reflectance features related to Arctic percent vegetation cover: Implications for hyperspectral remote sensing of Arctic tundra. Remote Sensing of Environment, 192, 58–72. https://doi.org/10.1016/j.rse.2017.02.002

Main-Knorn M, Pflug B, Louis J, Debaecker V, Müller-Wilm U, & Gascon F 2017. Sen2Cor for Sentinel-2. Image and Signal Processing for Remote Sensing XXIII, 10427, 37-48.

https://doi.org/10.1117/12.2278218

Marcial-Pablo M de J, Gonzalez-Sanchez A, Jimenez-Jimenez S I, Ontiveros-Capurata R E, & Ojeda-Bustamante W 2019. Estimation of vegetation fraction using RGB and multispectral images from UAV. International Journal of Remote Sensing, 40(2), 420–438.

https://doi.org/10.1080/01431161.2018.1528017

Marteinsdóttir B, Þórarinsdóttir E, Halldórsson G, Stefánsson J, Þórsson J, Svavarsdóttir K,

- Finnsdóttir R, & Jónsdóttir S 2021. GróLind - Sustainable Land Use Based on Ecological Knowledge. IGC Proceedings (2001-2023). https:// uknowledge.uky.edu/igc/24/1/25
- McGovern T H, Vésteinsson O, Fridriksson A, Church M, Lawson I, Simpson I A, Einarsson A, Dugmore A, Cook G, Perdikaris S, Edwards K J, Thomson A M, Adderley W P, Newton A, Lucas G, Edvardsson R, Aldred O, & Dunbar E 2007. Landscapes of Settlement in Northern Iceland: Historical Ecology of Human Impact and Climate Fluctuation on the Millennial Scale. American Anthropologist, 109(1), 27–51.

https://doi.org/10.1525/aa.2007.109.1.27

Meyer G E, & Neto J C 2008. Verification of color vegetation indices for automated crop imaging applications. Computers and Electronics in Agriculture, 63(2), 282–293.

https://doi.org/10.1016/j.compag.2008.03.009

Myers-Smith I H, Kerby J T, Phoenix G K, Bjerke J W, Epstein H E, Assmann J J, John C, Andreu-Hayles L, Angers-Blondin S, Beck P S A, Berner L T, Bhatt U S, Bjorkman A D, Blok D, Bryn A, Christiansen C T, Cornelissen J H C, Cunliffe A M, Elmendorf S C, ... Wipf S 2020. Complexity revealed in the greening of the Arctic. Nature Climate Change, 10(2), Article 2. https://doi.org/10.1038/s41558-019-0688-1

Nota E.W., Nijland W., de Haas T. 2022. Improving UAV-SfM time-series accuracy by co-alignment and contributions of ground control or RTK positioning. International Journal of Applied Earth Observation and Geoinformation, 109 (102772). https://doi.org/10.1016/j.jag.2022.102772

- Ólafsdóttir R, Schlyter P, & Haraldsson H V 2001. Simulating Icelandic Vegetation Cover during the Holocene Implications for Long-Term Land Degradation. Geografiska Annaler. Series A, Physical Geography, 83(4), 203–215.
- Poesen J 2018. Soil erosion in the Anthropocene: Research needs. Earth Surface Processes and Landforms, 43(1), 64-84.

https://doi.org/10.1002/esp.4250

- QGIS Development Team 2009. OGIS Geographic Information System [Computer software]. Open Source Geospatial Foundation. http://qgis.org
- Qi J, Chehbouni A, Huete A R, Kerr Y H, & Sorooshian S 1994. A modified soil adjusted

vegetation index. Remote Sensing of Environment, 48(2), 119–126.

https://doi.org/10.1016/0034-4257(94)90134-1

- R Core Team 2022. R: A Language and Environment for Statistical Computing [Computer software]. R Foundation for Statistical Computing. https://www.R-project.org/
- Riihimäki H, Luoto M, & Heiskanen J 2019. Estimating fractional cover of tundra vegetation at multiple scales using unmanned aerial systems and optical satellite data. *Remote Sensing of Environment*, 224, 119–132.

https://doi.org/10.1016/j.rse.2019.01.030

- Sentinel-2 Global Mosaic service 2014. https://s2gm.land.copernicus.eu/
- **Sepuru T K, & Dube T 2018.** An appraisal on the progress of remote sensing applications in soil erosion mapping and monitoring. *Remote Sensing Applications: Society and Environment*, *9*, 1–9. https://doi.org/10.1016/j.rsase.2017.10.005
- Shiferaw H, Bewket W, & Eckert S 2019. Performances of machine learning algorithms for mapping fractional cover of an invasive plant species in a dryland ecosystem. *Ecology and Evolution*, 9(5), 2562–2574.

https://doi.org/10.1002/ece3.4919

Streeter R T, & Cutler N A 2020. Assessing spatial patterns of soil erosion in a high-latitude rangeland. Land Degradation & Development, 31(15), 2003–2018.

https://doi.org/10.1002/ldr.3585

Tang C, Liu Y, Li Z, Guo L, Xu A, & Zhao J 2021. Effectiveness of vegetation cover pattern on regulating soil erosion and runoff generation in red soil environment, southern China. *Ecological Indicators*, 129, 107956.

https://doi.org/10.1016/j.ecolind.2021.107956

- **Thórhallsdóttir TE 1997.** Tundra ecosystems of Iceland. *Ecosystems of the World: Polar and Alpine Tundra*, 152–163.
- **Tsuyuzaki S, & Titus J H 1996.** Vegetation development patterns in erosive areas on the pumice plains of Mount St. Helens: American Midland Naturalist. *American Midland Naturalist*, 135, 172–177.

https://doi.org/10.2307/2426883

Tucker C J 1979. Red and photographic infrared linear combinations for monitoring vegetation.

- Remote Sensing of Environment, 8(2), 127–150. https://doi.org/10.1016/0034-4257(79)90013-0
- Ullmann T, Schmitt A, Roth A, Duffe J, Dech S, Hubberten H-W, & Baumhauer R 2014. Land Cover Characterization and Classification of Arctic Tundra Environments by Means of Polarized Synthetic Aperture X- and C-Band Radar (PolSAR) and Landsat 8 Multispectral Imagery—Richards Island, Canada. *Remote Sensing*, 6(9), Article 9. https://doi.org/10.3390/rs6098565
- Ullmann T, & Stauch G 2020. Surface Roughness Estimation in the Orog Nuur Basin (Southern Mongolia) Using Sentinel-1 SAR Time Series and Ground-Based Photogrammetry. *Remote Sensing*, 12(19), Article 19.

https://doi.org/10.3390/rs12193200

- Vieira A, & Rodrigues S C 2021. Soil Erosion: Current Challenges and Future Perspectives in a Changing World. BoD – Books on Demand.
- **Virtanen T, & Ek M 2014.** The fragmented nature of tundra landscape. *International Journal of Applied Earth Observation and Geoinformation*, *27*, 4–12. https://doi.org/10.1016/j.jag.2013.05.010
- Wadoux A M J C, Heuvelink G B M, de Bruin S, Brus D J 2021. Spatial cross-validation is not the right way to evaluate map accuracy. *Ecological Modelling*, 457, 109692.

https://doi-org./10.1016/j.ecolmodel.2021.109692

Wang Y, Yang Z, Kootstra G, & Khan H A 2023. The impact of variable illumination on vegetation indices and evaluation of illumination correction methods on chlorophyll content estimation using UAV imagery. *Plant Methods*, 19(1), 51.

https://doi.org/10.1186/s13007-023-01028-8

Xiao J, & Moody A 2005. A comparison of methods for estimating fractional green vegetation cover within a desert-to-upland transition zone in central New Mexico, USA. *Remote Sensing of Environment*, 98(2), 237–250.

https://doi.org/10.1016/j.rse.2005.07.011

Zhongming W, Lees B G, Feng J, Wanning L, & Haijing S 2010. Stratified vegetation cover index: A new way to assess vegetation impact on soil erosion. *CATENA*, 83(1), 87–93.

https://doi.org/10.1016/j.catena.2010.07.006

Recieved 29.11.2024 Accepted 15.10.2025